Comprehensive Analysis of Brain Tissue Using Focused Ion Beam Scanning Electron Microscopy (FIB-SEM): A Methodological Approach

Christine Martin[1], Elena Niggetiedt[1], Tina Hagena[1], Ann Kathrin Bergmann[2], Max Anstötz[1]

[1]Institute of Anatomy II, Medical Faculty, Heinrich-Heine-University, Düsseldorf, Germany
[2]Core Facility, Electron Microscopy, Heinrich-Heine-University, Düsseldorf, Germany

Background

Developed in the 1980s, focused ion beam scanning electron microscopy (FIB-SEM) technology has traditionally been utilised in materials science. Recently, however, it has gained significant traction in the life sciences, particularly for the examination of a diverse array of organ tissues. This method enables the recording of several thousand serial sections at nanometer resolution, thus enabling three-dimensional (3D) reconstructions and enhancing our understanding of cellular and subcellular structures. Acquisition and analysis processes, however, have to be optimised and partial developed from scratch.

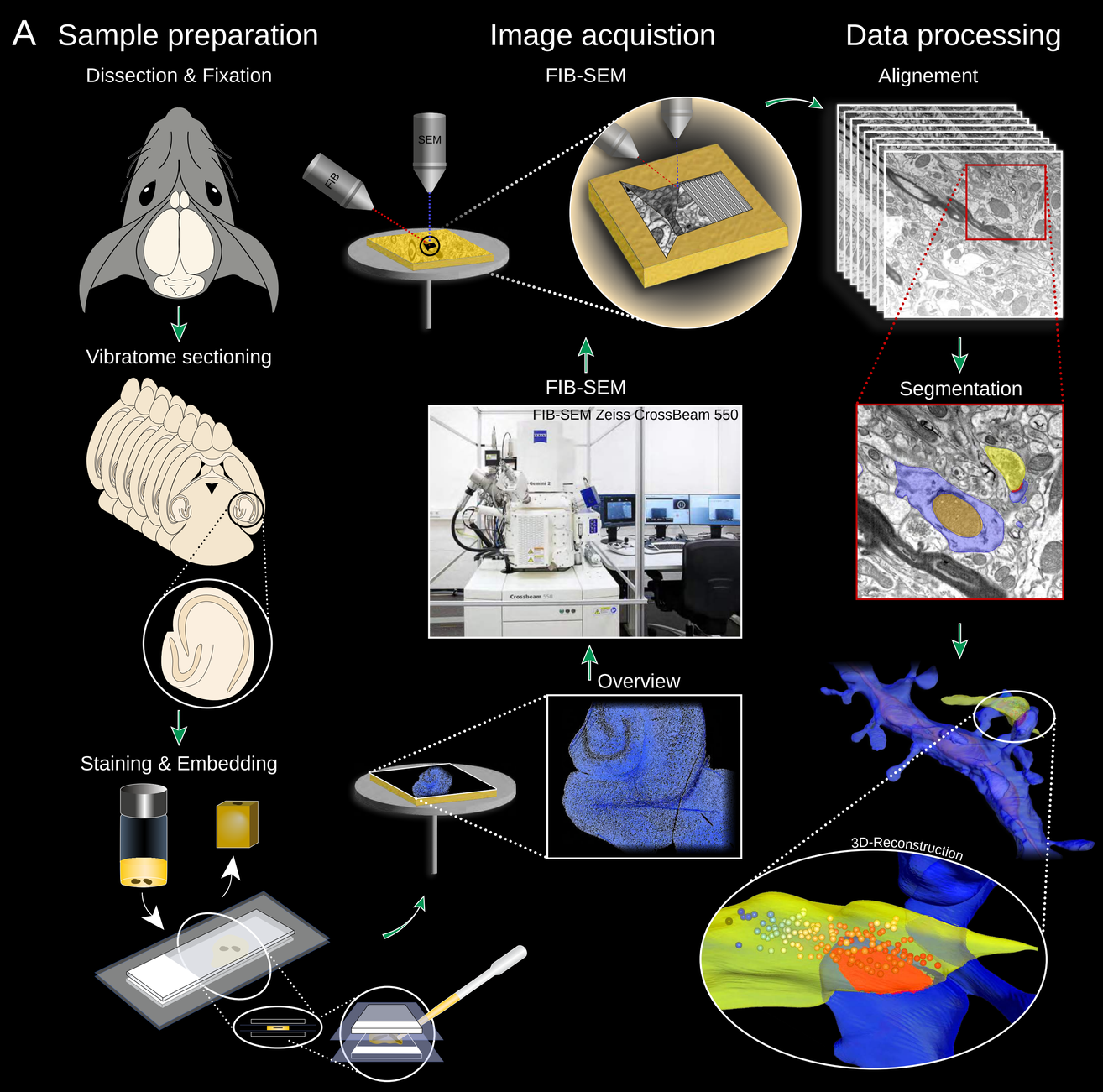

Methods

In our research group, we employ the FIB-SEM technique to gain detailed insights into the morphology of neuronal networks in the murine hippocampal formation. To develop and validate new methodological approaches in sample preparation, acquisition, post-processing analysis and statistics, we generate image stack from the murine Stratum Radiatum (SR) in CA1 and the outer molecular layer (OML) of the dentate gyrus (Figure 1).

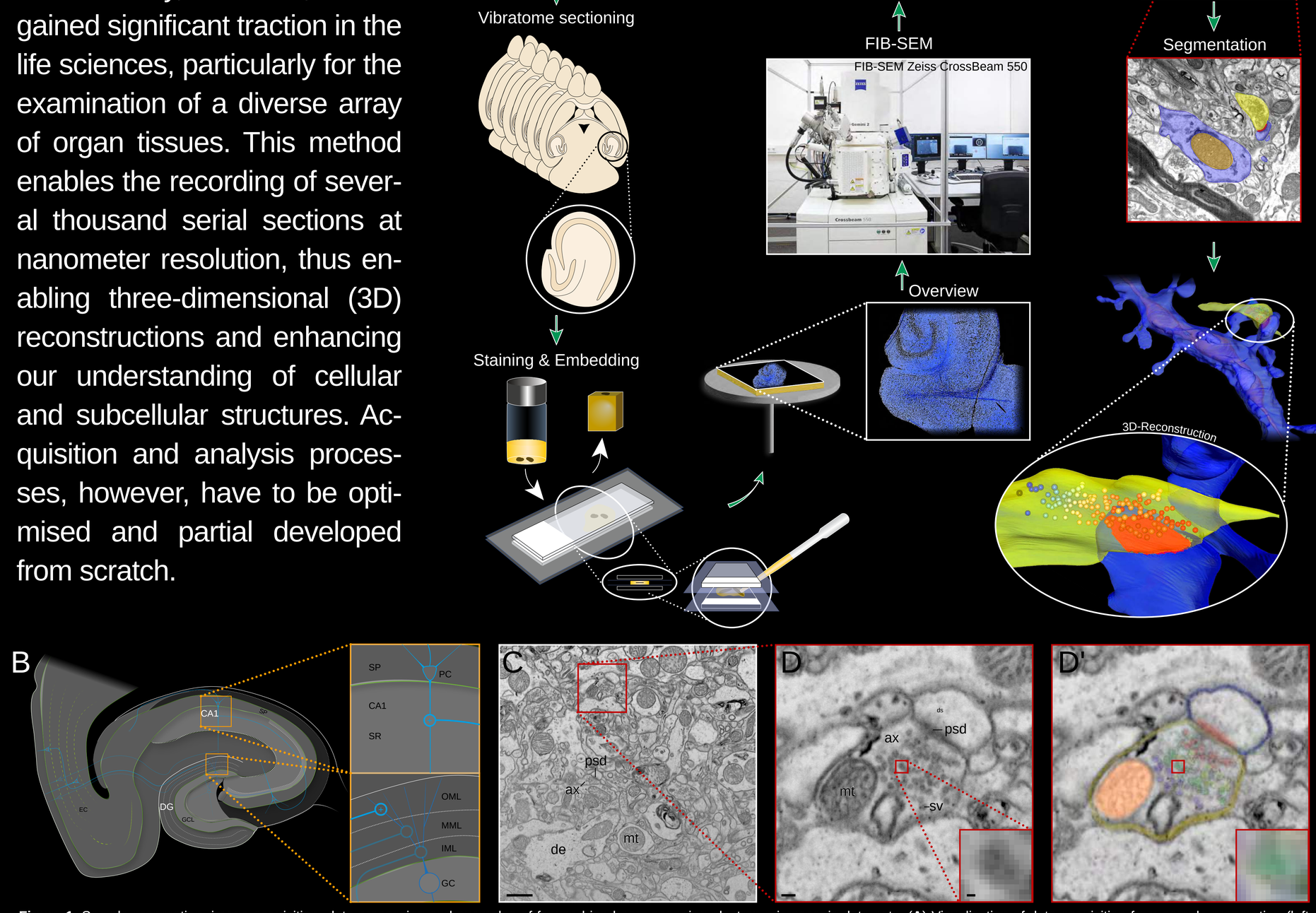

Figure 1. Sample preparation, image acquisition, data processing and examples of focused ion beam scanning electron microscopic data sets. (**A**) Visualisation of data acquisition from sample preparation (left column), image acquisition (middle column) and data processing (right column) for three-dimensional reconstruction of FIB-SEM based data sets. (**B**) Schematic diagram illustrating the murine hippocampus and its connectivity intrahippocampal as well as to the entorhinal cortex. Orange squares indicate the investigated regions in the CA1 region (upper inset) and the outer molecular layer of the dentate gyrus (lower inset). (**C**) Single plane of FIB-SEM data set. (**D**) Inset of region indicated in **C** showing an axonal bouton adjacent to a dendritic spine. Inset depicts a single synaptic vesicle. (**D'**) Same as D with highlighted axon (yellow), its synaptic vesicles (colour coded from blue to red) and mitochondrion (orange) and a dendritic spine (blue) with its postsynaptic density (red). Abbreviations: ax, axon; CA1, cornu ammonis 1; de, dendrite; ds, dendritic spine; DG, dentate gyrus; EC, entorhinal cortex; GC, granule cell; GCL, granule cell layer; IML, inner molecular layer; MML, middle molecular layer; mt, mitochondrion; OML, outer molecular layer; PC, pyramidal cell; psd, postsynaptic density; SP, stratum pyramidale; SR, stratum radiatum; sv, synaptic vesicle. Scale bars: 1 µm (C); 100 nm (D); 10 nm (inset).

Postsynapse

Figure 3 (***below***). Postsynaptic analyses of FIB-SEM generated data sets. (**A**) Three-dimensional reconstructions of dendrites and (**B**, **C**) its spine variations in two different hippocampal regions (CA1 [**B**] and dentate gyrus [**C**]). (**D**) Tubular analysis developed for spine examination (left). Distances from skeleton (blue tube) to spine surface (red spheres) are calculated for 10 different spine segments, thus allowing for a head to neck ratio analysis. Graph of segmental spine radius from CA1 (blue) and DG (black) region (right). Repeated measures two-way ANOVA on ranks (**E**) Postynaptic analyses displaying differences in spine length (left), albeit a lack of significant differences of spine volume (middle) in CA1 and dentate gyrus regions. Abbreviations: DG, dentate gyrus; CA1, cornu ammonis 1. Scale bars: 200 nm.

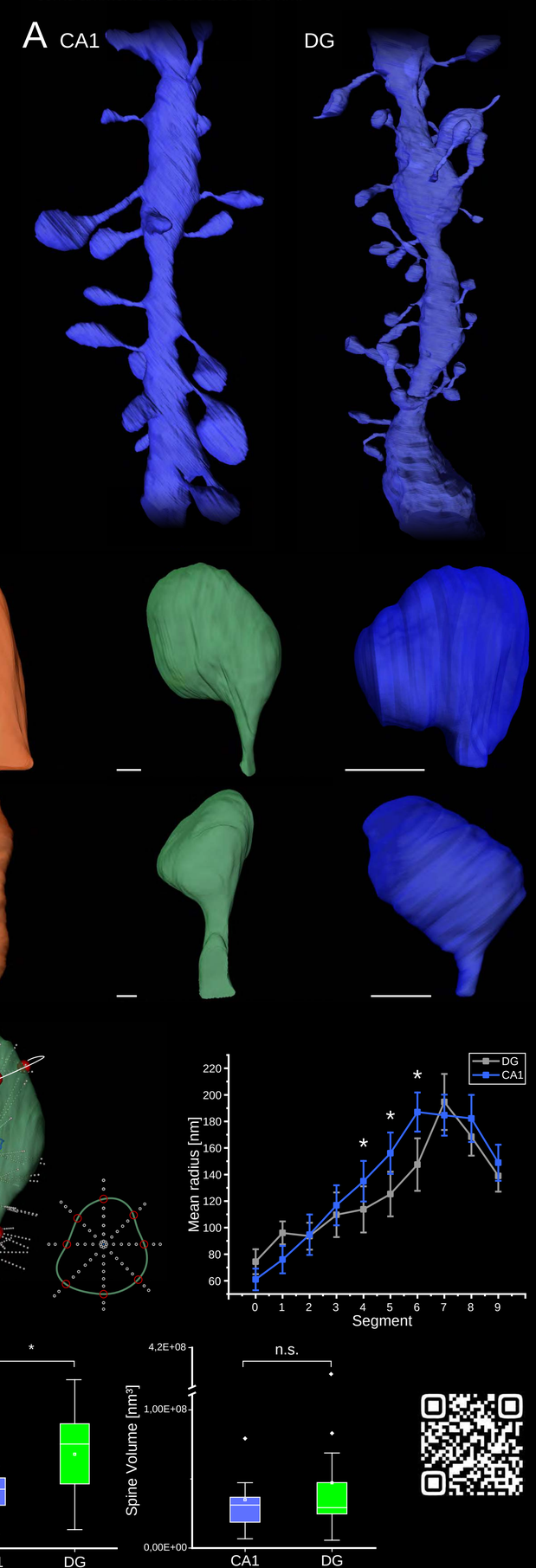

Presynapse

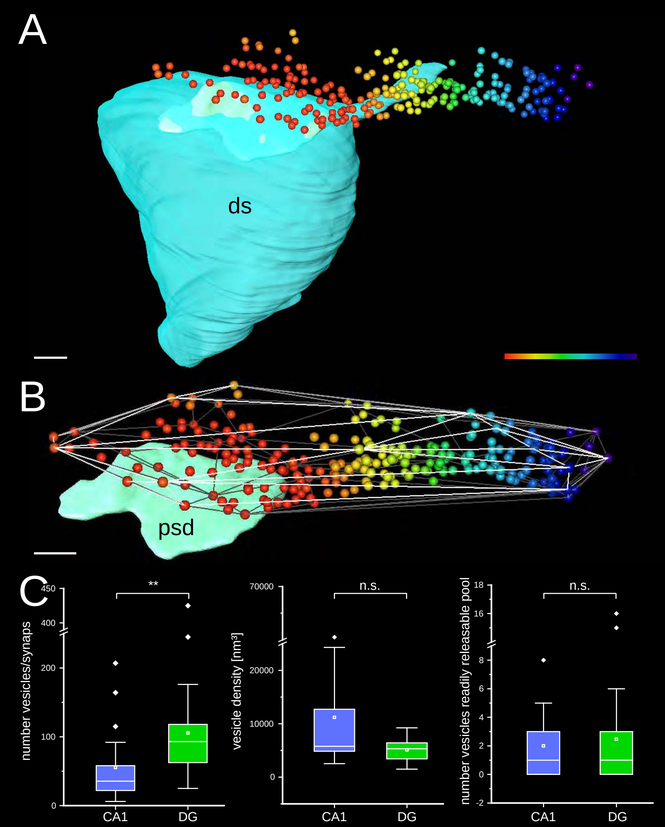

Figure 2. Presynaptic analyses of FIB-SEM generated data sets. (**A**) Presynaptic vesicles are visualised using a point cloud (colour-coded; 50 [red]–1000 [blue] nm). Colour codes indicate distances of vesicles to postsynaptic density. (**B**) Convex hull analyses (indicated by white lines) utilised for vesicle density calculation. (**C**) Various presynaptic analyses displaying differences of vesicle number per synapsve (left), albeit a lack of significant differences of vesicle number per µm³ (middle) as well as number of vesicles in close proximity to presynaptic membrane (readily releasable pool; right) in two different hippocampal regions (CA1 and DG). Abbreviations: DG, dentate gyrus; ds, dendritic spine, psd, postsynaptic density. Scale bars: 200 nm.

Results

Initially, we optimised all phases necessary for generating the corresponding data sets including sample preparation, acquisition settings, and 3D reconstruction setup. These methodological optimisations allow the investigation of the data sets in a manner that directly addresses specific research questions, such as (I) dendritic and spine 3D-morphology, (II) axonal 3D-morphology, (III) the number and size of subcellular structures, such as synaptic vesicles, postsynaptic densities and mitochondria (Figure 2 and 3).

Discussion

This approach provides the opportunity to explore additional scientific topics, including developmental changes or comparisons of different brain regions. Furthermore, it enables, in the future, the comparison of our data with those from disease models with neurological dysfunctions.

Acknowledgement

We are grateful to the Core Facility Electron Microscopy of the university clinic Düsseldorf for their support with electron microscopy imaging.

Funding

This study was supported by a grant from the German Research Fundation (DFG: 418317105) to UKD/HHU and Medical Faculty of HHU to EN.